BIOCHEMICAL PHARMACOLOGY 76 (2008) 249–257

available at www.sciencedirect.com

ScienceDirect

journal homepage: www.elsevier.com/locate/biochempharm

In vitro characterisation of human renal and hepatic frusemide glucuronidation and identification of the UDP-glucuronosyltransferase enzymes involved in this pathway

Oranun Kerdpin [a,b], *Kathleen M. Knights* [a], *David J. Elliot* [a], *John O. Miners* [a,*]

[a] *Department of Clinical Pharmacology, Flinders University, Adelaide, Australia*
[b] *Department of Pharmacy Practice, Naresuan University, Phitsanulok, Thailand*

ARTICLE INFO

Article history:
Received 6 March 2008
Accepted 24 April 2008

Keywords:
Frusemide
Glucuronidation
UDP-glucuronosyltransferase
Human kidney
Human liver

ABSTRACT

In order to gain insights into the renal and hepatic glucuronidation of frusemide (FSM), this study: (i) characterised the kinetics of FSM glucuronidation by human liver microsomes (HLM) and human kidney cortical- (HKCM) and medullary- (HKMM) microsomes, and (ii) identified the human UDP-glucuronosyltransferase enzyme(s) involved in this pathway. HLM, HKCM and HLMM efficiently glucuronidated FSM. FSM glucuronide (FSMG) formation followed Michaelis–Menten kinetics in all tissues. While the mean K_m for FSMG formation by HKMM (386 ± 68 μM) was lower than the K_m values for HLM (988 ± 271 μM) and HKCM (704 ± 278 μM), mean V_{max}/K_m values were comparable for the three tissues. A panel of recombinant UGT enzymes was screened for the capacity to glucuronidate FSM. UGT 1A1, 1A3, 1A6, 1A7, 1A9, 1A10 and 2B7 metabolised FSM. Of the renally and hepatically expressed enzymes, comparison of kinetic parameters suggests a predominant role of UGT1A9 in FSM glucuronidation, although UGT1A1 may also contribute to FSMG formation by HLM. Consistent with these observations, the UGT1A selective inhibitors phenylbutazone and sulfinpyrazone decreased FSMG formation by HLM, HKCM and HKMM by 60–80%, whereas the UGT2B7 selective inhibitor fluconazole reduced FSM glucuronidation by $\leq$20%. The ability of HKCM and HKMM to form FSMG supports the proposition that the kidney is the main organ involved in FSM glucuronidation in vivo, although a role for hepatic metabolism remains a possibility in renal dysfunction. The data further demonstrate the potential importance of both the medulla and cortex in renal drug metabolism and detoxification.

© 2008 Elsevier Inc. All rights reserved.

1. Introduction

The anthranilic acid derivative frusemide (FSM) (Fig. 1) is a potent diuretic which acts via blockade of active sodium/potassium and chloride reabsorption in the thick ascending limb of the loop of Henle [1]. FSM, which is employed primarily in the treatment of oedema associated with renal impairment, congestive cardiac failure and hepatic cirrhosis, ranks amongst the most widely used clinical drugs. By way of example, in 2006 approximately 1.4 million and 10.5 million prescriptions for FSM were dispensed in Australia and England, respectively (http://www.medicareaustralia.gov.au; http://www.ic.nhs.uk/webfiles/publications/pca2006/). Available evidence indicates that

* *Corresponding author at*: Department of Clinical Pharmacology, Flinders University School of Medicine, Flinders Medical Centre, Bedford Park, SA 5042, Australia. Tel.: +61 8 82044131; fax: +61 8 82045114.
E-mail address: john.miners@flinders.edu.au (J.O. Miners).
0006-2952/$ – see front matter © 2008 Elsevier Inc. All rights reserved.
doi:10.1016/j.bcp.2008.04.014

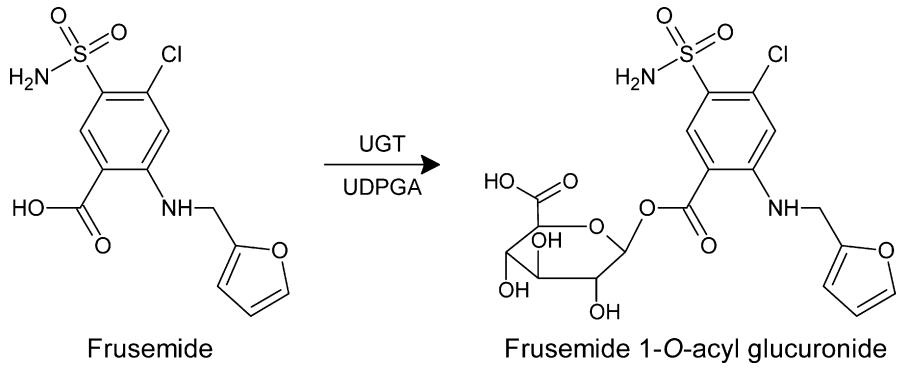

Fig. 1 – Structures of frusemide (FSM) and frusemide 1-O-acyl glucuronide (FSMG).

glucuronidation, resulting in the formation of FSM 1-O-acyl glucuronide (FSMG) (Fig. 1), is the major if not sole biotransformation pathway of FSM in humans [2]. Although renal excretion of unchanged drug is the predominant clearance mechanism of FSM in healthy subjects [3], the ratio of FSMG to FSM excreted in urine is significant ranging from 0.21 to 0.31 [4]. While it appears that FSM glucuronidation in humans and the rabbit occurs primarily in the kidney [2–6], renal dysfunction results in markedly increased fecal excretion of FSM (at the expense of urinary excretion of FSM and FSMG) [6,7]. Potentially, this may arise from biliary excretion of FSM itself or hepatically formed FSMG (with subsequent hydrolysis in the gastrointestinal tract).

Glucuronidation reactions are catalysed by the enzyme UDP-glucuronosyltransferase (UGT) and involve the covalent linkage of glucuronic acid, derived from the cofactor UDP-glucuronic acid (UDPGA), to a nucleophilic atom on the substrate. UGT exists as a superfamily of enzymes that exhibit distinct but overlapping substrate selectivities [8]. Nineteen human UGT proteins that utilize UDPGA as cofactor have been identified to date, and these have been classified into two families (UGT1 and UGT2) based on sequence identity [9]. The liver is the major site of glucuronidation. However, a number of extrahepatic tissues exhibit significant UGT activity [10]. Importantly, both UGT1A and UGT2B7 enzymes are known to be expressed in kidney cortex and medulla, including the proximal and distal convoluted tubules, the loops of Henle, and the collecting ducts [11]. Moreover, glucuronidation activity by human renal tissue has been demonstrated towards numerous xenobiotics and endogenous compounds [11–20].

Despite the widespread use of FSM and its clinical utilization over four decades, the comparative roles of kidney and liver in human FSM glucuronidation appear not to have been characterised. Furthermore, the UGT enzymes contributing to FSMG formation are yet to be elucidated. This study compared the kinetics of FSM glucuronidation by human liver microsomes (HLM) and both human kidney cortical- (HKCM) and medullary- (HKMM) microsomes to gain insights into hepatic and renal FSM metabolism. In addition, microsomal inhibition approaches and activity measurements with recombinant UGTs were employed to identify the human UGT enzyme(s) that potentially contribute to FSMG formation.

2. Materials and methods

Alamethicin (from *Trichoderma viride*), β-glucuronidase (from *Escherichia coli*), FSM, UDP-glucuronic acid (UDPGA; trisodium salt), phenylbutazone, sulfinpyrazone and zidovudine (3′-azido-3′-deoxythymidine) were purchased from Sigma–Aldrich (Sydney, Australia). Fluconazole was a gift from Pfizer Australia (Sydney, Australia). All other reagents and solvents were of analytical reagent grade.

2.1. Human liver and kidney microsomes

Human livers (HL 7, 10, 12, 29, and 40) were obtained from the human liver bank of the Department of Clinical Pharmacology, Flinders Medical Centre. Approval was obtained from the Flinders Medical Centre Clinical Research Ethics Committee and from the donor next-of-kin for the procurement and use of human liver tissue in xenobiotic metabolism studies. Microsomes were prepared by differential centrifugation, as described by Bowalgaha et al. [21], and stored at −80 °C until use. Similarly, human kidney tissues (HK 6, 7, 9, and 10) from subjects who had undergone radical nephrectomy for malignant disease were obtained from the joint Flinders Medical Centre/Repatriation General Hospital Tissue Bank. Approvals for tissue collection and in vitro xenobiotic metabolism studies were obtained from the Research Ethics Committees of the Repatriation General Hospital and the Flinders Medical Centre. Renal cortical and medullary tissue distant to the primary tumor were isolated from fresh kidneys immediately following surgery. HKCM and HKMM were prepared by differential centrifugation, as described by Tsoutsikos et al. [19], and stored at −80 °C until use. Renal and hepatic microsomes were activated by preincubation with alamethicin (50 μg/mg protein) on ice for 30 min prior to use in incubations [22].

2.2. Expression of UGT proteins

UGT 1A1, 1A3, 1A4, 1A6, 1A7, 1A8, 1A9, 1A10, 2B4, 2B7, 2B15, 2B17, and 2B28 cDNAs were stably expressed in a human embryonic kidney cell line (HEK293), as described previously [23,24]. Cells were separately transfected with the individual UGT cDNAs cloned into the pEF-IRES-puro6 expression vector and incubated at 37 °C in Dulbecco's modified Eagle's medium, which contained puromycin (1 mg/l), 10% fetal calf serum, and

penicillin G (100 units/ml)/streptomycin (100 μg/ml) in a humidified incubator with an atmosphere of 5% CO_2. After growth to at least 80% confluence, cells were harvested and washed in phosphate-buffered saline. Cells were subsequently lysed by sonication using a Vibra Cell VCX130 Ultrasonic Processor (Sonics and Materials, Newtown, CT, USA) set to an amplitude of 40%. Cells expressing UGT1A proteins were sonicated with four 2 s 'bursts', each separated by 1 min cooling on ice. A similar method was applied to UGT2B subfamily enzymes, except that sonication was limited to 1 s bursts due to the greater instability of these proteins to sonication. Lysed samples were centrifuged at 12,000 × *g* for 1 min at 4 °C, and the supernatant fraction was separated and stored at −80 °C until use. Expression of each UGT protein was demonstrated by immunoblotting with a commercial UGT1A antibody and a non-selective UGT antibody (raised against purified mouse UGT) [24]. Activities of recombinant UGTs (except UGT1A4) were confirmed using the non-selective substrate 4-methylumbelliferone, as described by Rowland et al. [25]. The activity of recombinant UGT1A4 was demonstrated using trifluoperazine as substrate [26].

2.3. FSM glucuronidation assay

Incubation mixtures, in a total volume of 200 μl, contained either activated HLM, HKCM or HKMM (0.4 mg/ml) or HEK293 cell lysate expressing recombinant UGT (1 mg/ml), UDPGA (5 mM), $MgCl_2$ (4 mM), and FSM in 0.1 M phosphate buffer (pH 7.4). Incubation tubes were protected from light by aluminium foil. The kinetics of FSM glucuronidation were characterised using 9–12 substrate concentrations in the ranges: 25–3000 μM for HLM, HKCM, HKMM, UGT1A1, and UGT1A9; 125–3500 μM for UGT1A6; 250–8000 μM for UGT1A3; and 500–6000 μM for UGT2B7. After a 5 min preincubation at 37 °C, reactions were initiated by the addition of UDPGA. Incubations were carried out for 60 min at 37 °C in a shaking water bath. Separate 'blank' incubations were performed in the absence of UDPGA. Reactions were terminated by the addition of ice-cold 4% acetic acid/96% methanol (200 μl) and centrifugation at 4000 × *g* for 10 min. An aliquot of the supernatant fraction was injected onto an Agilent 1100 HPLC system (Agilent Technologies, Palo Alto, CA, USA). Chromatography was performed using a Waters Nova-Pak C18 column (150 × 3.9 mm, 4 μm; Milford, MA, USA) with a Phenomenex SecurityGuard cartridge (Phenomenex, Torrance, CA, USA). Peaks were separated with 73% 10 mM triethylamine, pH 2.5 (adjusted with $HClO_4$) and 27% acetonitrile. The mobile phase flow rate was 1.0 ml/min and peaks were monitored by UV detection at 340 nm. Under these conditions, retention times for FSMG and FSM were 3.3 and 8.8 min, respectively. FSMG was quantified by comparison of peak areas to those of an FSM external standard curve prepared over the concentration range of 1–10 μM. FSM standard curves were linear over this concentration range, with r^2 values > 0.99. The lower limit of quantification, defined as 5-times background (with an injection volume of 75 μl) was 0.08 μM, equivalent to a product formation rate of 1.4 pmol/min mg. Overall within-day assay reproducibility was assessed by measuring FSMG formation in five separate incubations of the same batch of HLM. Within-day coefficients of variation were 2.5% and 0.7% for substrate concentrations of 200 and 2500 μM, respectively. The formation of FSMG was linear with incubation times to at least 75 min and microsomal protein concentrations to at least 1 mg/ml.

The identity of the FSMG peak formed by incubations of HLM, HKCM, HKMM and recombinant UGTs was confirmed by enzymatic hydrolysis. A 200 μl FSM glucuronidation incubation mixture (see above) was terminated with 85% H_3PO_4 (5 μl) and centrifuged (12,000 × *g* for 10 min). The supernatant fraction was decanted and adjusted to pH 6 with 1 M KOH. Enzymatic hydrolysis was performed by incubation with β-glucuronidase (10 units/ml) at 37 °C for 2 h. Control incubations without β-glucuronidase were performed simultaneously.

To assess the stability of FSMG, an incubation containing FSM (3000 μM) and HLM was scaled up to a volume of 3 ml. After incubation at 37 °C for 60 min, the sample was treated with H_3PO_4 (85%, 50 μl) to precipitate microsomal protein. The sample was centrifuged (4,000 × *g* for 10 min), the supernatant fraction collected and the pH adjusted to 7.4 by the dropwise addition of KOH (2M). A 200 μl aliquot of the mixture was collected prior to and after 10, 15, 20, 30, 40, 50 and 60 min incubation at 37 °C. Samples were treated as described above for incubations of FSM, and then FSMG was measured by HPLC.

2.4. Inhibition of FSM glucuronidation by fluconazole, zidovudine, phenylbutazone and sulfinpyrazone

Inhibition of FSM glucuronidation, at a substrate concentration of 1000 μM (the approximate K_m for this reaction catalysed by HLM; see Section 3) was investigated using pooled HLM, pooled HKCM, pooled HKMM, and recombinant UGT1A1, UGT1A9 and UGT2B7. Concentrations of fluconazole, zidovudine, phenylbutazone and sulfinpyrazone employed in the inhibition studies were 2.5, 2.5, 1, and 1 mM, respectively [26–28].

2.5. Data analysis

Data points represent the mean of duplicate estimates (variance < 10%). Kinetic constants for FSM glucuronidation by HLM, HKCM, HKMM and recombinant UGTs were obtained by fitting experimental data to the Michaelis–Menten and substrate inhibition equations using EnzFitter (Biosoft, Cambridge, UK).

Michaelis–Menten equation:

$$v = \frac{V_{max} \times [S]}{K_m + [S]}$$

where v is the rate of reaction, V_{max} is the maximum velocity, K_m is the Michaelis constant (substrate concentration at 0.5 V_{max}), and [S] is the substrate concentration.

Substrate inhibition:

$$v = \frac{V_{max}}{1 + (K_m/[S]) + ([S]/K_{si})}$$

where K_{si} is the constant describing the substrate inhibition interaction.

Goodness of fit to kinetic models was assessed by comparison of the *F*-statistic, coefficient of determination (r^2), parameter standard errors, and 95% confidence intervals.

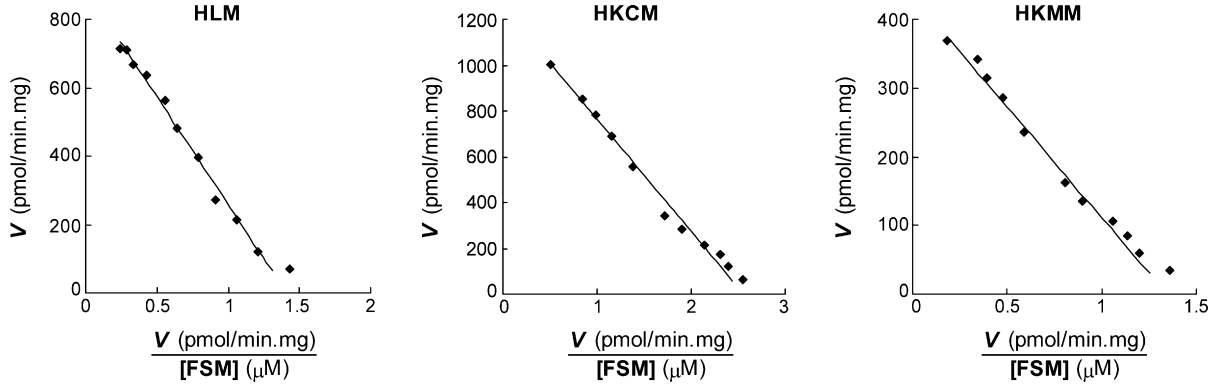

Fig. 2 – Representative Eadie–Hofstee plots for frusemide glucuronidation by: human liver microsomes (HL40); human kidney cortical microsomes (HK9); and human kidney medullary microsomes (HK9). Points are experimentally determined values (means of duplicate measurements at each concentration), while the solid lines are the computer-generated curves of best fit.

Kinetic constants are reported as the parameter ± standard error of the parameter estimate.

2.6. *Statistics*

Statistical analysis (Univariate General Linear Model with Tukey post hoc analysis) of kinetic constants for FSMG formation by HLM, HKMM and HKCM was performed using SPSS for Windows (SPSS Inc, Chicago).

3. Results

3.1. *FSM glucuronidation by human liver and kidney microsomes*

HPLC analysis of incubations containing FSM and UDPGA revealed a metabolite peak with a retention time of 3.3 min, which was not observed in incubations performed without UDPGA or FSM. The identity of the FSMG peak was confirmed by hydrolysis with β-glucuronidase, which resulted in a loss of the peak eluting at 3.3 min in the chromatogram. There was no evidence of peaks corresponding to β-glucuronidase resistant rearrangement products following hydrolysis. The stability of FSMG at pH 7.4 over 60 min was assessed according to the procedure described in Section 2.3. The area of the FSMG peak was reduced by only 2.8% over 60 min when incubated at 37 °C (pH 7.4). The coefficient of variation of the FSMG peak area following incubation for 10, 15, 20, 30, 40, 50 and 60 min was 2.5%.

FSM glucuronidation exhibited Michaelis–Menten kinetics in all five livers and four kidneys investigated (Fig. 2). Kinetic parameters for FSMG formation by HLM, HKMM and HKCM are shown in Table 1. As noted previously, standard curves were prepared using FSM. Thus, rates of FSM glucuronide formation and V_{max} values for this metabolite should therefore be

Table 1 – Derived kinetic parameters for frusemide glucuronidation by human liver and kidney microsomes

	Kinetic parameters[a]		
	V_{max} (pmol/min mg)	K_m (μM)	V_{max}/K_m (μl/min mg)
Human liver microsomes			
HL7	968 ± 23	1084 ± 48	0.9
HL10	417 ± 3	802 ± 13	0.5
HL12	1412 ± 25	1307 ± 49	1.1
HL29	500 ± 1	1121 ± 4	0.4
HL40	887 ± 4	627 ± 8	1.4
Human kidney microsomes			
HK6, cortex	928 ± 13	913 ± 25	1.0
HK6, medulla	274 ± 2	336 ± 6	0.8
HK7, cortex	125 ± 1	439 ± 8	0.3
HK7, medulla	329 ± 4	443 ± 14	0.7
HK9, cortex	1256 ± 1	491 ± 1	2.6
HK9, medulla	432 ± 1	320 ± 2	1.4
HK10, cortex	1344 ± 26	974 ± 32	1.4
HK10, medulla	266 ± 0.4	446 ± 2	0.6

[a] K_m and V_{max} reported as parameter ± S.E. of parameter fit.

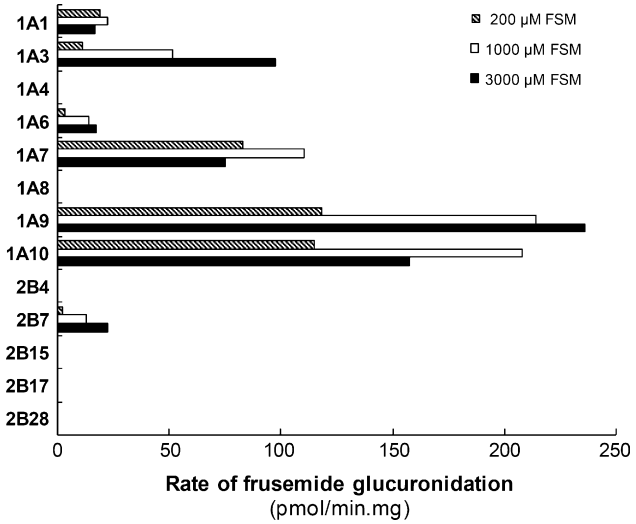

Fig. 3 – Formation of frusemide glucuronide by recombinant UDP-glucuronosyltransferases at substrate concentrations of 200, 1000, and 3000 μM. Results represent the means of duplicate estimations.

considered 'apparent'. Mean (±S.D.) derived K_m values for HLM, HKCM and HKMM were 988 ± 271, 704 ± 278 and 386 ± 68 μM, respectively. Only the difference between the K_m values for HLM and HKMM was statistically significant ($p < 0.05$), although the small sample size (four kidneys) may obscure a 'real' difference between HKCM and HKMM ($p = 0.17$). Mean (±S.D.) derived V_{max} values for FSMG formation by HLM, HKCM and HKMM were 837 ± 400, 913 ± 555 and 325 ± 77 pmol/min mg, respectively. Differences were not statistically significant but, as noted above, this probably reflects the small sample size and wide variability in this parameter. Notably, V_{max} values for FSMG formation by HKCM varied 11-fold between the four kidneys.

3.2. *FSM glucuronidation by recombinant human UGTs*

UGT 1A1, 1A3, 1A4, 1A6, 1A7, 1A8, 1A9, 1A10, 2B4, 2B7, 2B15, 2B17, and 2B28 were screened for FSM glucuronidation activity at substrate concentrations of 200, 1000, and 3000 μM. Of the recombinant UGT enzymes, UGT 1A1, 1A3, 1A6, 1A7, 1A9, 1A10, and 2B7 converted FSM to its 1-O-acyl glucuronide. UGT1A9 and UGT1A10 exhibited the highest activity (Fig. 3). UGT1A7 and UGT1A10 appear to be expressed only in the gastrointestinal tract [10] and hence cannot contribute to FSM glucuronidation by HLM or human kidney microsomes. Thus, kinetic studies were subsequently performed only with UGT 1A1, 1A3, 1A6, 1A9, and 2B7. Kinetic data for UGT1A9 and UGT2B7 were well modelled by the Michaelis–Menten equation while data for UGT1A1, UGT1A3, and UGT1A6 were best fitted to the substrate inhibition equation (Table 2). Substrate inhibition was weak with UGT1A1 ($K_{si} > > K_m$), but potent for UGT1A3 and UGT1A6 ($K_{si} < < K_m$). Eadie–Hofstee plots for each enzyme are shown in Fig. 4.

3.3. *Inhibition of FSM glucuronidation by fluconazole, zidovudine, phenylbutazone, and sulfinpyrazone*

The selective UGT2B7 inhibitor fluconazole (2.5 mM) [27] decreased FSMG formation by pooled HLM, pooled HKCM, and pooled HKMM by ≤20% at an FSM concentration of 1000 μM, whereas approximately 80% inhibition was observed with UGT2B7 as the positive control (Fig. 5). Similar results were obtained using the known UGT2B7 substrate zidovudine (2.5 mM) [29] as the inhibitor of FSM glucuronidation (Fig. 5). On the other hand, phenylbutazone (1 mM) and sulfinpyrazone (1 mM), known selective substrates of UGT1A9 and non-selective inhibitors of UGT1A enzymes [26,28,30], exhibited 60–80% inhibition of FSMG formation by pooled HLM, pooled HKCM, and pooled HKMM, and 75–95% inhibition of FSM glucuronidation by recombinant UGT1A9 (Fig. 5). Phenylbutazone and sulfinpyrazone also inhibited UGT1A1 catalysed glucuronidation by 40–85% (Fig. 5).

4. Discussion

This study demonstrates that HLM, HKMM and HKCM efficiently glucuronidate FSM. Ranges of intrinsic clearances (V_{max}/K_m) for each tissue were comparable. These data concur with the similarities in S-naproxen glucuronidation by HLM, HKMM and HKCM reported previously by this group [11,20]. The glucuronidation of FSM by HKMM and HKCM is consistent with the reported expression of UGT1A and UGT2B7 enzymes in human kidney [11–13]. Expression was shown recently to occur along the entire length of the human nephron, but was absent in the glomerulus, Bowman's capsule and the renal

Table 2 – Derived kinetic parameters for frusemide glucuronidation by UGT 1A1, 1A3, 1A6, 1A9 and 2B7

	Kinetic parameters[a]			
	V_{max} (pmol/min mg)	K_m (μM)	K_{si} (μM)	V_{max}/K_m (μl/min mg)
UGT1A1[b]	42 ± 1	141 ± 9	3796 ± 369	0.3
UGT1A3[b]	1914 ± 3	36033 ± 120	560 ± 2	0.05
UGT1A6[b]	836 ± 27	47279 ± 1866	94 ± 5	0.02
UGT1A9[c]	288 ± 3	242 ± 8	–	1.2
UGT2B7[c]	43 ± 1	2022 ± 61	–	0.02

[a] K_m, K_{si} and V_{max} reported as parameter ± S.E. of parameter fit.
[b] Substrate inhibition kinetics.
[c] Michaelis–Menten kinetics.

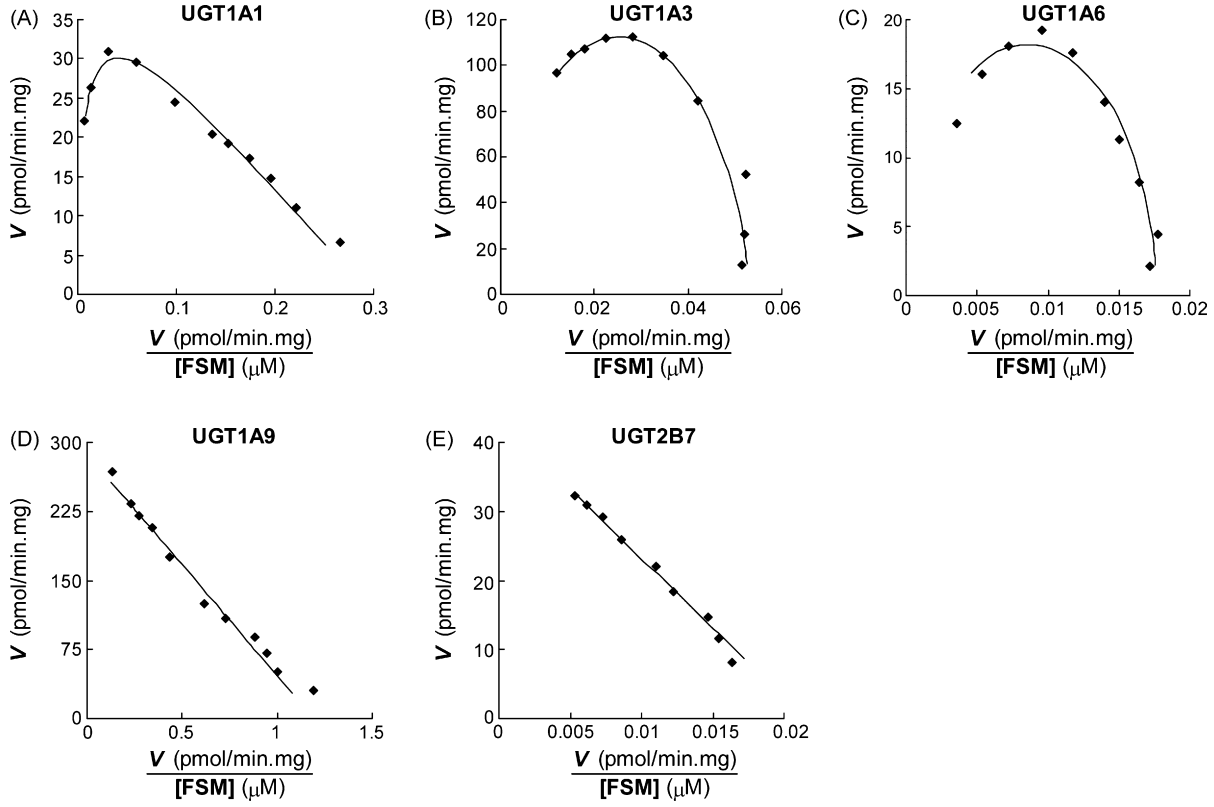

Fig. 4 – Eadie–Hofstee plots for frusemide glucuronidation by recombinant UGTs: (A) UGT1A1; (B) UGT1A3; (C) UGT1A6; (D) UGT1A9 and (E) UGT2B7. Points are experimentally determined values (means of duplicate measurements at each concentration), while the solid lines are the computer-generated curves of best fit.

vasculature [11]. Apart from FSM and S-naproxen, microsomes prepared from human kidney tissue (medulla plus cortex) have been shown to glucuronidate numerous drugs and chemicals including other non-steroidal anti-inflammatory drugs (NSAIDs; e.g. fenamates, ketoprofen), gemfibrozil, 4-methylumbelliferone, morphine, mycophenolic acid, naloxone, propofol and valproic acid [12–20]. Although the overall contribution of the kidney to the metabolic clearance of drugs is unknown, these data indicate that the both medulla and cortex may contribute to 'local' drug and chemical detoxification in this organ. Conversely, the formation of reactive acyl glucuronides and/or inhibition of renal drug glucuronidation may be relevant to the development of NSAID-induced nephrotoxicity [20].

K_m values for FSMG formation by HLM and HKCM were in a similar range and varied approximately 2-fold in each of these tissues. Interestingly, K_m values generated using HKMM were lower and showed less variability (1.4-fold) than HLM and HKCM. This may reflect a different contribution of UGT1A enzymes to FSM glucuronidation in HKMM. The K_m values reported here for FSM glucuronidation are almost certainly overestimates, given the likely important contribution of UGT1A9 to FSMG formation (see below). Long-chain unsaturated fatty acids released from the membranes of HLM and HEK293 cells during the course of an incubation are known to act as potent competitive inhibitors of UGT1A9 and UGT2B7 [19,31,32]. The addition of bovine serum albumin or fatty acid free serum albumin to incubations sequesters the inhibitory fatty acids, resulting in an approximate 10-fold reduction in K_m values (based on unbound substrate concentration) [31,32]. Thus, the 'true' K_m values for microsomal FSM glucuronidation are likely to be in the range of 30–130 μM. It should be noted that the extensive binding of FSM to albumin (fraction unbound in plasma is <2%, [3]) precluded the addition of bovine- or human-serum albumin to incubations in this work.

UGT 1A1, 1A3, 1A6, 1A9, 2B7 and 2B15 have all been reported to glucuronidate carboxylic acids [33]. However, UGT1A9 and UGT2B7 appear to be most commonly associated with this reaction. Here, recombinant UGT 1A1, 1A3, 1A6, 1A7, 1A9, 1A10 and 2B7 (expressed in HEK293 cells) metabolised FSM. UGT1A7 and UGT1A10 appear to be expressed solely or predominantly in the gastrointestinal tract [10] and their capacity to glucuronidate FSM is consistent with previous observations of drug and chemical glucuronidation by intestinal microsomes, for example [14,17,18]. In contrast to data presented here, Cheng et al. [34] reported that UGT1A8 glucuronidated FSM, while UGT1A10 lacked activity towards this substrate. The reason for the difference between the studies is not clear, although Cheng et al. noted that the sequence of the UGT1A8 cDNA employed in their work differed from other published sequences.

Of the hepatically and renally expressed enzymes, K_m values for FSMG formation by UGT 1A3, 1A6 and 2B7 were approximately 2- to 36-fold higher than the highest K_m values

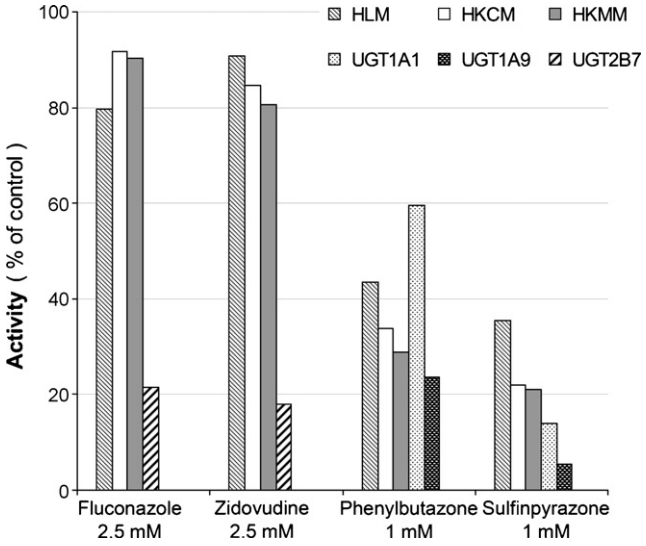

Fig. 5 – Effects of fluconazole (2.5 mM), zidovudine (2.5 mM), phenylbutazone (1 mM), and sulfinpyrazone (1mM) on frusemide glucuronidation by pooled human liver microsomes, pooled human kidney cortical microsomes, pooled human kidney medullary microsomes, and UGT 2B7, 1A1, and 1A9. Each bar represents the mean percentage activity relative to control from duplicate measurements. Fluconazole and zidovudine inhibited UGT1A enzyme activities by <20%, and phenylbutazone and sulfinpyrazone inhibited UGT2B7 activity by <15% (data not shown).

observed for HLM, HKCM and HKMM. Furthermore, unlike the microsomal glucuronidation reactions, potent substrate inhibition was observed with UGT1A3 and UGT1A6. In contrast, the K_m values for FSM glucuronidation by UGT1A1 and UGT1A9 were below the ranges observed for hepatic and renal microsomes. It is important to note, however, that K_m values determined with recombinant UGT1A9 and UGT2B7 (but not UGT1A1) are typically 3- to 4-fold lower than those for the corresponding glucuronidation reaction catalysed by HLM (and presumably kidney microsomes) due to the lower content of inhibitory long chain unsaturated fatty acids present in expression systems [31,32,35]. Hence, correspondence of K_m values generated using HLM (and HKM) and recombinant enzymes is not expected for UGT1A9 and UGT2B7 catalysed reactions.

Although UGT1A1 is expressed in liver, this enzyme appears not to be expressed in kidney [10,12,13]. Of the enzymes found here to glucuronidate FSM, UGT 1A3, 1A6, 1A9 and 2B7 are known to exist in human kidney. Thus, on the basis of the comparative kinetic data, UGT1A9 would appear to be primarily responsible for renal FSMG formation. The higher intrinsic clearance observed with UGT1A9 further suggests a greater role for this enzyme in FSM glucuronidation compared to UGT1A1 in HLM, although the level of expression of UGT1A9 is 50% higher than that of UGT1A1 in the HEK293 cells employed here [24]. Inhibition experiments confirmed a predominant role of UGT1A enzymes in FSM glucuronidation by HLM, HKMM, and HKCM. Fluconazole, a selective inhibitor of UGT2B7 [27], and zidovudine, a selective substrate of UGT2B7 [29,36], inhibited the microsomal reactions by $\leq$20%. In contrast, sulfinpyrazone and phenylbutazone, which are selective substrates of UGT1A9 but non-selective UGT1A inhibitors [26,28,30], inhibited FSMG formation by HLM, HKMM and HKCM by 60% to 80%.

As noted above, K_m values for FSMG formation generated using HKMM were lower and showed less variability (1.4-fold) than HLM and HKCM. This might be taken to suggest the involvement of multiple enzymes in FSM glucuronidation by HLM and HKCM. Since the inhibition data (Fig. 5) suggest a minor role at best for UGT2B7, the possibility remains that another unidentified enzyme contributes to FSMG formation in these tissues. UGT1A1, UGT1A9 and UGT2B7 all exhibit genetic polymorphism [37–41], and this may contribute to the variability in renal and hepatic FSM glucuronidation observed here.

Although renal excretion of unchanged drug is the main pathway of FSM elimination in humans, metabolic clearance via glucuronidation is significant. In a review of FSM pharmacokinetics, the proportion of an intravenous dose excreted in urine as unchanged FSM was reported to range from 59% to 66% in healthy subjects [4]. Mean FSMG to FSM urinary ratios were 0.21–0.31, with one study reporting a range of 8–30% for the proportion of the FSM dose excreted in urine as FSMG. Interestingly, co-administration of FSM and pentopril, an angiotensin converting enzyme inhibitor, to healthy volunteers caused a 3-fold increase in urinary FSMG excretion [42]. It was proposed that this effect arises from inhibition of the luminal transport of FSM by pentopril, with enhanced availability of FSM for intrarenal glucuronidation. Indeed, available evidence indicates that the proportion of the FSM dose excreted in urine as FSMG arises from renal glucuronidation [5,6]. The formation of FSMG by HKMM and HKCM reported here is consistent with renal FSM glucuronidation in vivo.

Fecal excretion of FSM increases substantially in patients with renal failure, at the expense of urinary excretion of FSM and FSMG [6,7]. Given the similar intrinsic clearances for FSM glucuronidation by HLM, HKMM and HKCM observed here, it might be speculated that fecal excretion arises from biliary excretion of hepatically formed FSMG and subsequent hydrolysis (by β-glucuronidase) in the gastrointestinal tract. However, Valentine et al. [43] failed to detect a β-glucuronidase sensitive metabolite in the intestinal perfusate of healthy volunteers administered FSM.

In summary, FSM was efficiently glucuronidated by HLM, HKMM and HKCM. UGT1A9 appears to be the main enzyme responsible for FSMG formation in these tissues, although there may also be a contribution of UGT1A1 in liver. The glucuronidation of FSM by HKMM and HKCM is consistent with in vivo observations implicating the kidney as the organ responsible for the formation of FSMG excreted in urine. The ability of both HKMM and HKCM to glucuronidate FSM further supports the notion that renal UGT enzymes play an important role in drug and chemical detoxification in the kidney, and may additionally contribute significantly to xenobiotic clearance. Hepatic FSM glucuronidation (and subsequent biliary elimination of FSMG) may be of importance in renal failure patients, but direct evidence for this is lacking.

Acknowledgements

This work was funded by a grant from the National Health and Medical Research Council of Australia. The authors acknowledge the assistance of Mr Daniel Caruana in the development of the HPLC assay for FSMG and Dr Paraskevi Gaganis for the preparation of human kidney microsomes.

REFERENCES

[1] Brater DC. Clinical pharmacology of loop diuretics. Drugs 1991;41(Suppl 3):14–22.
[2] Boles Ponto LL, Schoenwald RD. Furosemide (frusemide)—A pharmacokinetic/pharmacodynamic review (part I). Clin Pharmacokinet 1990;18:381–408.
[3] Smith DE, Lin ET, Benet LZ. Absorption and disposition of furosemide in healthy volunteers, measured with a metabolite-specific assay. Drug Metab Dispos 1980;8: 337–42.
[4] Hammarlund-Udenaes M, Benet LZ. Frusemide pharmacokinetics and pharmacodynamics in health and disease – An update. J Pharmacokinet Biopharmceut 1989;17:1–46.
[5] Pichette V, du Souich P. Role of the kidneys in the metabolism of furosemide: its inhibition by probenecid. J Am Soc Nephrol 1996;7:345–9.
[6] Smith DE, Benet LZ. Biotransformation of furosemide in kidney transplant patients. Eur J Clin Pharmacol 1983;24:787–90.
[7] Beermann B, Dalen E, Lindstrom B. Elimination of furosemide in healthy subjects and in those with renal failure. Clin Pharmacol Ther 1977;22:70–8.
[8] Miners JO, Smith PA, Sorich MJ, McKinnon RA, Mackenzie PI. Predicting human drug glucuronidation parameters: application of in vitro and in silico modeling approaches. Annu Rev Pharmacol Toxicol 2004;44:1–25.
[9] Mackenzie PI, Bock KW, Burchell B, Guillemette C, Ikushiro S, Iyanagi T, et al. Nomenclature update for the mammalian UDP glycosyltransferase (UGT) gene superfamily. Pharmacogenet Genomics 2005;15:677–85.
[10] Tukey RH, Strassburg CP. Human UDP-glucuronosyltransferases: metabolism, expression, and disease. Annu Rev Pharmacol Toxicol 2000;40: 581–616.
[11] Gaganis P, Miners JO, Brennan JS, Thomas A, Knights KM. Human renal cortical and medullary UDP-glucuronosyltransferases (UGTs): immunohistochemical localization of UGT2B7 and UGT1A enzymes and kinetic characterization of S-naproxen glucuronidation. J Pharmacol Exp Ther 2007;323:422–30.
[12] Sutherland L, Ebner T, Burchell B. The expression of UDP-glucuronosyltransferases of the UGT1 family in human liver and kidney and in response to drugs. Biochem Pharmacol 1993;45:295–301.
[13] McGurk KA, Brierley CH, Burchell B. Drug glucuronidation by human renal UDP-glucuronosyltransferases. Biochem Pharmacol 1998;55:1005–12.
[14] Raoof AA, van Obbergh LJ, de Ville de Goyet J, Verbeeck RK. Extrahepatic glucuronidation of propofol in man: possible contribution of gut wall and kidney. Eur J Clin Pharmacol 1996;50:91–6.
[15] Hiraoka H, Yamamoto K, Miyoshi S, Morita T, Nakamura K, Kadoi Y, et al. Kidneys contribute to the extrahepatic clearance of propofol in humans, but not lungs and brain. Br J Clin Pharmacol 2005;60:176–82.
[16] Soars MG, Riley RJ, Findlay KA, Coffey MJ, Burchell B. Evidence for significant differences in microsomal drug glucuronidation by canine and human liver and kidney. Drug Metab Dispos 2001;29:121–6.
[17] Bowalgaha K, Miners JO. The glucuronidation of mycophenolic acid by human liver, kidney and jejunum microsomes. Br J Clin Pharmacol 2001;52:605–9.
[18] Soars MG, Burchell B, Riley RJ. In vitro analysis of human drug glucuronidation and prediction of in vivo metabolic clearance. J Pharmacol Exp Ther 2002;301: 382–90.
[19] Tsoutsikos P, Miners JO, Stapleton A, Thomas A, Sallustio BC, Knights KM. Evidence that unsaturated fatty acids are potent inhibitors of renal UDP-glucuronosyltransferases (UGT): kinetic studies using human kidney cortical microsomes and recombinant UGT1A9 and UGT2B7. Biochem Pharmacol 2004;67:191–9.
[20] Gaganis P, Miners JO, Knights KM. Glucuronidation of fenamates: kinetic studies using human kidney cortical microsomes and recombinant UDP-glucuronosyltransfearse (UGT) 1A9 and 2B7. Biochem Pharmacol 2007;73:1683–91.
[21] Bowalgaha K, Elliot DJ, Mackenzie PI, Knights KM, Swedmark S, Miners JO. *S*-Naproxen and desmethylnaproxen glucuronidation by human liver microsomes and recombinant human UDP-glucuronosyltransferases (UGT): role of UGT2B7 in the elimination of naproxen. Br J Clin Pharmacol 2005;60: 423–33.
[22] Boase S, Miners JO. In vitro–in vivo correlations for drugs eliminated by glucuronidation: investigations with the model substrate zidovudine. Br J Clin Pharmacol 2002;54:493–503.
[23] Stone AN, Mackenzie PI, Galetin A, Houston JB, Miners JO. Isoform selectivity and kinetics of morphine 3- and 6-glucuronidation by human udp-glucuronosyltransferases: evidence for atypical glucuronidation kinetics by UGT2B7. Drug Metab Dispos 2003;31:1086–9.
[24] Uchaipichat V, Mackenzie PI, Guo XH, Gardner-Stephen D, Galetin A, Houston JB, et al. Human UDP-glucuronosyltransferases: isoform selectivity and kinetics of 4-methylumbelliferone and 1-naphthol glucuronidation, effects of organic solvents, and inhibition by diclofenac and probenecid. Drug Metab Dispos 2004;32:413–23.
[25] Rowland A, Elliot DJ, Williams JA, Mackenzie PI, Dickinson RG, Miners JO. In vitro characterization of lamotrigine *N*2-glucuronidation and the lamotrigine–valproic acid interaction. Drug Metab Dispos 2006;34:1055–62.
[26] Uchaipichat V, Mackenzie PI, Elliot DJ, Miners JO. Selectivity of substrate (trifluoperazine) and inhibitor (amitriptyline, androsterone, canrenoic acid, hecogenin, phenylbutazone, quinidine, quinine, and sulfinpyrazone) ''probes'' for human UDP-glucuronosyltransferases. Drug Metab Dispos 2006;34:449–56.
[27] Uchaipichat V, Winner LK, Mackenzie PI, Elliot DJ, Williams JA, Miners JO. Quantitative prediction of in vivo inhibitory interactions involving glucuronidated drugs from in vitro data: the effect of fluconazole on zidovudine glucuronidation. Br J Clin Pharmacol 2006;61:427–39.
[28] Kerdpin O, Elliot DJ, Mackenzie PI, Miners JO. Sulfinpyrazone *C*-glucuronidation is catalyzed selectively by human UDP-glucuronosyltransferase 1A9. Drug Metab Dispos 2006;34:1950–3.
[29] Court MH, Krishnaswamy S, Hao Q, Duan X, Patten CJ, von Moltke LL, et al. Evaluation of 3'-azido-3'-deoxythymidine, morphine, and codeine as probe substrates for UDP-glucuronosyltransferase 2B7 (UGT2B7) in human liver microsomes: specificity and influence of the UGT2B7*2 polymorphism. Drug Metab Dispos 2002;31:1125–33.

[30] Nishiyama T, Kobori T, Arai K, Ogura K, Ohnuma T, Ishii K, et al. Identification of human UDP-glucuronosyltransferase isoform(s) responsible for the C-glucuronidation of phenylbutazone. Arch Biochem Biophys 2006;454:72–9.
[31] Rowland A, Gaganis P, Elliot DJ, Mackenzie PI, Knights KM, Miners JO. Binding of inhibitory fatty acids is responsible for the enhancement of UDP-glucuronosyltransferase 2B7 activity by albumin: implications for in vitro–in vivo extrapolation. J Pharmacol Exp Ther 2007;321:137–47.
[32] Rowland A, Knights KM, Mackenzie PI, Miners JO. The 'albumin effect' and drug glucuronidation: bovine serum albumin and fatty acid free human serum albumin enhance the glucuronidation of UGT1A9 substrates but not UGT1A1 and UGT1A6 activities. Drug Metab Dispos 2008;36:1056–62.
[33] Sorich MJ, McKinnon RA, Miners JO, Smith PA. The importance of local chemical structure for chemical metabolism by human uridine 5'-diphosphate – glucuronosyltransferase. J Chem Inf Model 2006;46:2692–7.
[34] Cheng Z, Radominska-Pandya A, Tephly TR. Studies of the substrate specificity of human intestinal UDP-glucuronosyltransferases 1A8 and 1A10. Drug Metab Dispos 1999;27:1165–70.
[35] Court MH. Isoform selective probe substrates for in vitro studies of human UDP-glucuronosyltransferases. Methods Enzymol 2005;400:104–16.
[36] Miners JO, Knights KM, Houston JB, Mackenzie PI. In vitro–in vivo correlation for drugs and other compounds eliminated by glucuronidation in humans: pitfalls and promises. Biochem Pharmacol 2006;71:1531–9.
[37] Miners JO, McKinnon RA, Mackenzie PI. Toxicological significance of genetic polymorphisms of UDP-glucuronosyltransferase. Toxicology 2002;181–182: 453–6.
[38] Udomuksorn W, Elliot DJ, Lewis BC, Mackenzie PI, Yoovathaworn K, Miners JO. Influence of mutations associated with Gilbert and Crigler–Najjar type II syndromes on the glucuronidation kinetics of bilirubin and other UDP-glucuronosyltransferase 1A (UGT1A) substrates. Pharmacogenet Genomics 2007;17:1017–29.
[39] Bhasker CR, McKinnon WM, Stone AN, Kubota T, Ishizaki T, Miners JO. Genetic polymorphism of UDP-glucuronosyltransferase 2B7 (UGT2B7) at amino acid 268: ethnic diversity of alleles and potential clinical significance. Pharmacogenetics 2000;10:679–85.
[40] Girard H, Villeneuve L, Court MH, Fortier L-C, Caron P, Hao Q, et al. The novel UGT1A9 intronic I399 polymorphism appears as a predictor of 7-ethyl-10-hydroxycamptothecin glucuronidation levels in the liver. Drug Metab Dispos 2006;34:1220–8.
[41] Villeneuve L, Girard H, Fortier L-C, gagne J-F, Guillemette C. Novel functional polymorphisms in the UGT1A7 and UGT1A9 glucuronidating enzymes in Caucasian and African-American subjects and their impact on the metabolism of 7-ethyl-10-hydroxycamptothecin and flavopiridol anticancer drugs. J Pharmacol Exp Ther 2003;307:117–28.
[42] Rakhit A, Kochak GM, Tipnis V, Hurley ME. Inhibition of renal clearance of furosemide by pentopril, an angiotensin converting enzyme inhibitor. Clin Pharmacol Ther 1987;41:580–6.
[43] Valentine JF, Brater DC, Krejs GJ. Clearance of furosemide by the gastrointestinal tract. J Pharmacol Exp Ther 1986;236:177–80.